Journal of Applied Polymer Science

Electrospinning of Chitosan/Poly(lactic acid) Nanofibers: The Favorable Effect of Nonionic Surfactant

Xiaoqian Shan,[1] Fengqian Li,[2] Changsheng Liu,[3] Qun Gao[1]

[1]School of Materials Science & Engineering, Shanghai Institute of Technology, Shanghai 201418, People's Republic of China
[2]Department of Pharmaceutics, Shanghai Xuhui Dahua Hospital, Shanghai 200237, People's Republic of China
[3]The State Key Laboratory of Bioreactor Engineering, East China, University of Science and Technology, Shanghai 200237, People's Republic of China
Correspondence to: X. Shan (E-mail: shanxiaoqian@sit.edu.cn)

ABSTRACT: To improve the electrospinnability of chitosan (CS), a series of nanofiber membrane blends comprised of CS, poly(lactic acid) (PLA), and nonionic surfactant polyoxyethylene nonylphenol ether (TX-15), were made. Uniform nanofibers with no bead-like structures were obtained from solutions of 2% TX-15 with 6% CS(50)/PLA(50). The diameter was between 200 and 300 nm. We found that with increasing TX-15 in the blend, the nanofibers displayed more hydrophilicity. Compared to CS/PLA nanofibers, the blend polymers with TX-15 had better tensile mechanical properties. Finally, all cells examined showed high levels of attachment and spreading on CS/PLA/TX-15 nanofibers with a TX-15 content of 0∼3%. Thus, the nanofibers were nontoxic. In conclusion, adding PLA and TX-15 to CS via solution-blending and electrospinning may be an effective way to toughen CS nanofibers and make them more suitable for drug delivery or tissue engineering applications. © 2014 Wiley Periodicals, Inc. J. Appl. Polym. Sci. **2014**, *131*, 41098.

KEYWORDS: biocompatibility; biomaterials; electrospinning; nanostructured polymers; polyesters

Received 23 February 2014; accepted 31 May 2014
DOI: 10.1002/app.41098

INTRODUCTION

Penetrating and extensive skin diseases represent some of the most devastating injuries affecting humans.[1] Traditional therapies are limited by a number of problems, including donor site shortage for autologous skin transplantation and frequent scarring.[2] Skin tissue engineering is an emerging field aimed at addressing these challenges associated with the treatment of skin disease, burns, soft tissue trauma, and disease leading to skin necrosis.[3] In contrast to conventional medical therapies, skin tissue engineering aims to mimic the natural extracellular matrix (ECM), providing a suitable environment for cells. Thus, the artificial ECM should represent a hospitable environment in which cells can grow and behave as if in their natural setting.[4,5] The use of synthetic, biodegradable, and biocompatible tissue scaffolds has facilitated research efforts in this direction.[6]

Naturally occurring ECM is comprised of an internal molecular network. Therefore, artificial ECM scaffolds must mimic this structure, and most are comprised of interconnected pores and nanofibers[7] Electrospinning is a well-established fiber-spinning technique, which is driven by an electric force and produces nanofibers from polymer solutions or melts.[8] Once electrostatic forces overcome the surface tension of the polymer solution or melts, the solution is ejected from the apex of the "Taylor cone." The solvent rapidly evaporates, and the charged jets of polymer solution are randomly deposited on the collector to form a porous nonwoven fabric.[9] Recently, there has been significant interest in the electrospinning of biodegradable polymers for use as scaffolds in tissue engineering since the continuous fibrous mats that are generated have high porosity, large surface areas, and resemble the structure of the ECM.[10–12]

Nanofibers have multiple biomedical applications, including tissue engineering, drug delivery, wound dressing, use as nanosensors, and the filtering of medium. The polymer must be biocompatible and have low toxicity.[9,13] Chitosan (CS) is a biopolymer produced by renewable resources and obtained from alkaline deacetylation of natural chitin. It has been widely used in biomedicine as a scaffold material for tissue engineering; this is, in large part, due to several of its characteristics, including biocompatibility, biodegradability, antibacterial properties, high affinity for *in vivo* macromolecules, and wound-healing activity.[14] Recent reports have described the successful electrospinning of chitosan (CS) and its derivatives into nanofibers from traditional acid solvent.[15,16] However, despite these successes, the spinning preparation process is hindered by the fact that CS is insoluble at neutral and alkaline pH; instead, it is soluble in acidic media. Thus, organic solvents or organic acid solvents,

Table I. Variation in Physicochemical Properties with Different Compositions of Samples

Samples	Solvents mixture and ratio	Polymers (w/v,%) (6%)	TX-15 (w/v,%)	Diameter (nm)	Viscosity (cP) at 25°C	Conductivity (μs) at 25°C	Dynamic swelling behavior (%)		Contact angles (°)
							24 h	72 h	
a	TFA : DCM : DMF = 1 : 1 : 1	PLA	0	935 ± 120	235	1328	30.6 ± 2.4	34.2 ± 1.5	83.1 ± 0.7
b		CS	0	-	378	2192	55.1 ± 4.1	57.8 ± 1.3	61.5 ± 1.0
c		PLA : CS = 1 : 1	0	450 ± 65	291	1741	39.1 ± 5.2	43.3 ± 3.6	71.8 ± 0.2
d			1	490 ± 83	216	1829	44.4 ± 3.1	48.0 ± 2.1	67.2 ± 0.1
e			2	249 ± 52	197	1972	52.7 ± 2.0	55.9 ± 2.8	59.9 ± 0.8
f			3	525 ± 59	229	2068	57.4 ± 1.8	59.6 ± 2.2	53.7 ± 0.7
g			4	863 ± 42	273	2154	62.4 ± 2.5	65.5 ± 1.4	41.5 ± 0.9

such as acetic acid or trifluoroacetic acid (TFA), must be used.[17–19] These organic solvents are toxic and can cause harm when applied directly to human skin or tissue; as a result, CS's application is limited.[20] Additionally, due to their hydrophilicity and solubility in acidic medium, CS nanofibers exhibit relatively low mechanical strength and a high degradation rate, resulting in poor electrospinnability[7] and unsatisfactory release behavior.[21] Therefore, it is necessary to investigate CS modifications that will improve its solubility and performance. To date, synthetic polyesters, such as poly(ε-caporlactone) (PCL), poly(lactic acid) (PLA), poly(glycolic acid) (PGA), poly(lactide-co-glycoside) (PLGA), and polyurethane, have attracted much attention for their biodegradability and biocompatibility in the human body.[22] Because of the inherent limitation of CS, it is often combined/blended with synthetic polymers to enhance its mechanical properties, decrease its degradation, and increase its affinity to cellular components.[23–26]

The aim of this study was to identify the most suitable electrospun scaffold for skin tissue engineering applications. We describe optimization of the electrospinning process and parameter preparation. We have characterized the scaffold properties by analyzing fiber diameter and morphology. We have also performed an in depth mechanical study, testing both tension and *in vitro* cell proliferation responses. In our preliminary work, we used electrospinning to prepare a nanofiber mat from a CS-PLA (50 : 50) solution but were unsuccessful. Therefore, we added polyoxyethylene nonylphenol ether (TX-15) to the blend system as a guest material in a different weight ratio. TX-15 is a nonionic surfactant. It may self-assemble to form colloidal aggregates, which are able to serve as solubilization factors to improve the solubility of polymers and deliver lypophilic functional ingredients. Incorporation of micelles into polymers may also modulate the molecular structure, alter rheological and interfacial properties of polymer dispersions,[27] and reduce the surface tension between the two polymers and increase their miscibilities.[28] This could represent a novel means to further functionalize biopolymer nanofibers. Nevertheless, very little has been reported on this application. Moreover, none of the studies provide a universal conclusion as to which of the investigated surfactant parameters enable a reliable prediction of fiber morphology of the electrospun product. The surfactant TX-15 is a new addition to the PLA/CS system; thus, it is necessary to investigate the biocompatibility of this new fiber system. Although a detailed physical characterization of CS and PLA blend nanofibers can be found in the literature, none of the reports have examined the biocompatibility of the mixture polymers with a surfactant in the presence of cultured cells *in vitro*. Thus, the effect of surfactant on polymer electrospinnability, fiber morphology, fibrous mechanical strength, and biocompatibility, are explored in this study.

MATERIALS AND METHODS

Materials

PDLLA (Mw = 200 kDa, D/L = 50/50) was purchased from Jinan Daigang Biomaterial Co. (China). Chitosan (degree of deacetylation 80–85%, Mw = 200 kDa) was purchased from Zhejiang Goalden-Shell Biochemical Co. (China). Solvents, including TFA, dichloromethane (DCM), and *n,n*-dimethyl formamide (DMF), and the nonionic surfactant Polyoxyethylene (15) nonylphenyl ether (TX-15) were all purchased from Sigma Aldrich. All solvents were of analytical quality. Reagents for *in vitro* biological testing were sourced as specified in the text below.

Preparation and Properties of Spinning Solutions

Four spinning solution series were used in this study: (a) PLA, (b) CS, (c) PLA/CS (1 : 1), and (d) PLA/CS/TX-15 (1–4%). Maintaining the same degree of solvation, solutions (a)–(c) of 6% polymer(s) were all prepared by dissolving 0.3 g of PLA or CS or the blend of PLA/CS (1 : 1) in 5 mL of TFA/DCM/DMF mixture (1 : 1 : 1). For solution series (d), the solvent mixture consists of the common solvents applied for the majority of compounds. Thus, the solution with TX-15 concentration of 1% was prepared by dissolving 0.05 g of TX-15 in 5 mL of solution (c) at room temperature. This solution was mixed well for 2 h. Similarly, the PLA/CS/TX-15 solutions with TX-15 concentrations of 2%, 3%, and 4% were prepared by dissolving 0.1, 0.15, and 0.2 g of TX-15, respectively, in 5 mL of solution (c). Detailed blending compositions for electrospinning solutions are shown in Table I.

For the conductivity measurements, the electrospinning solutions were measured by an electric conductivity meter (DDS-307, Shanghai. Precision & Scientific Instrument Co., China) at

25°C. The viscosity of the electrospinning solutions was measured by Brookfield viscometer (DV-II, Brookfield Engineering Laboratories). All the electrospinning solutions were kept at 25°C.

Scaffold Fabrication by Electronspinning

The electrospinning setup and procedure have been previously described.[9] Solutions were taken up in a 5-mL glass syringe equipped with a 20-gauge, stainless steel needle (diameter = 0.9 mm). The needle was connected to the emitting electrode of positive polarity of a Gamma High Voltage Research device. The electric potential was fixed at 25 kv. Nanofibers were collected on an aluminum sheet that was wrapped on a rotating collector. The solution was electrospun at 25°C with a flow rate of 1mL h^{-1}, and the collection distance was fixed at approximately 10 cm. The solution feed was driven both by gravity and the electrostatic force that was generated during spinning.

Characterization of Nanofibers

Morphology and diameter of nanofibers were determined using scanning electron microscopy (SEM) (S-3400N II, HITACHI, Japan). Samples on the aluminum foil were cut into small pieces and sputter-coated with platinum prior to SEM imaging. Based on SEM imaging, an average fiber diameter was determined from a minimum of 100 random nanofibers using previously described methods.[4,20]

The wettability of the fibrous mats was measured with a contact angle goniometer (JJC-1 static contact angle equipment; Changchun No. 5 Optical Instrument Co.) at room temperature. For each measurement, a droplet of deionized water (10 μL) was placed onto the membrane surface and the contact angle was measured.

The hydrophilicity of the nanofibers was determined by a dynamic swelling behavior measurement using a gravimetric method, as previously described.[29,30] Nanofibers were cut into squares (10–15 mg each) and then immersed in phosphate-buffered saline. The initial pH of all media was 7.4, and it remained between 7.4 and 8.0 (measured with a pH meter immediately after samples were removed) for the duration of the experiment. Fiber samples in duplicate were incubated in 10 mL of medium at 37°C in a non-CO_2 incubator (BPN-50CH (UV), Shanghai Yiheng Instruments Co., China). Samples were removed at preset time points up to 72 h (3 days), and the medium was changed daily for all remaining samples. The swollen weight (after blotting with tissue paper) and dried weight (after drying in a vacuum to constant weight) were recorded. Water uptake was calculated according to eq. (1):

$$\text{Water Uptake}(\%) = \frac{W_{\text{swollen}} - W_{\text{dry}}}{W_{\text{dry}}} \times 100\% \quad (1)$$

Mechanical Testing. The mechanical properties of the nanofibers were tested with a universal testing machine (Sun 500, Italy) with a load cell of 25 N. The mats were cut into dumbbell strips of 50 mm length and 10 mm width. All samples were tested under a crosshead speed of 2 mm/min at room temperature. The machine-recorded data were used to process the tensile stress–strain curves of the specimens. Specifically, the tensile strains were obtained by dividing the crosshead displacements by the original gauge length (30 mm). The average values were calculated from 10 results.

***In Vitro* Cell Adhesion and Proliferation.** Fiber cytotoxicity was determined by 3-(4,5-dimethylthiazol-2-yl)−2,5 -diphenyl-tetrazolium bromide (MTT assay) in human bone-marrow mesenchymal stem cell (hMSCs).[31]

Discs made from the electrospun nanofibers were attached to the bottom of a 96-well plate by spotting the well with DCM to create an adhesive surface; disks were then placed into the well. The solvent was thoroughly removed by drying in a vacuum overnight. To sterilize the disks, a 25% ethanol solution was added to each well for 10 min and successively replaced with a 50% and 75% ethanol solution for 10 min each.

Human bone-marrow MSC suspensions were dispensed into 96-well plates and incubated overnight to allow cells to attach. The fiber-scaffolds were seeded with 10,000 cells in 200 µL of culture medium. The cells were cultured up to 72 h and then culture medium was replaced with 100 µL of scaffold/culture medium suspensions at different concentrations at 37°C. After 72 h incubation, 30 µL of MTT solution was added into each well and incubated at 37°C for 4 h. The solution was then removed and 100 µL of dimethylsulfoxide (DMSO) was added to each well. The plate was incubated for 15 min at 37°C and optical densities (OD) at 490 nm were measured with a Spectra max PLUS384 device (Molecular Devices Corp.,). Cell viability was calculated by the following formula:

$$\text{Cellviability}(\%) = \frac{OD_{\text{sample}}}{OD_{\text{control}}} \times 100\% \quad (2)$$

SEM was used to examine the morphology of hMSC-seeded scaffolds. Samples were fixed in a 2.5% glutaraldehyde solution. They were dehydrated and sputter-coated with platinum for 5 min before imaging.

RESULTS AND DISCUSSION

Characterization of Nanofibers

Morphology and Diameter of Electrospun Fibrous Mats. SEM images of all different polymer compositions are shown in Figure 1. Using the 100% CS solution, it was difficult to obtain the desired nanofibers from electrospinning; instead of yielding a fibrous structure, pure CS gave lamellar or drop-like deposition on the rotating-collector [Figure 1(b)]. Previous reports have shown that fiber-forming facilitating additives, such as synthetic polymers,[7] can be used to improve the electrospinnability of CS. Here, we find that PLA is electrospun in a uniform structure [Figure 1(a)]. The addition of PLA dramatically alters the morphology of electrospun nanofibers and changes the CS film structure from lamellar in shape to the bead-like structure shown in Figure 1(c). After being blended with CS, the diameter of the PLA nanofibers significantly decreased from 935 ± 120 nm to 450 ± 65 nm (Table I). A previous publication suggested that, in polymer solutions, nonionic surfactants greatly reduce bead formation.[32] Despite this, in our study, we found that the addition of surfactant TX-15 to polymer solutions modified the electrospinning conditions of polymer blends by altering the surface properties of nanofibers to prevent

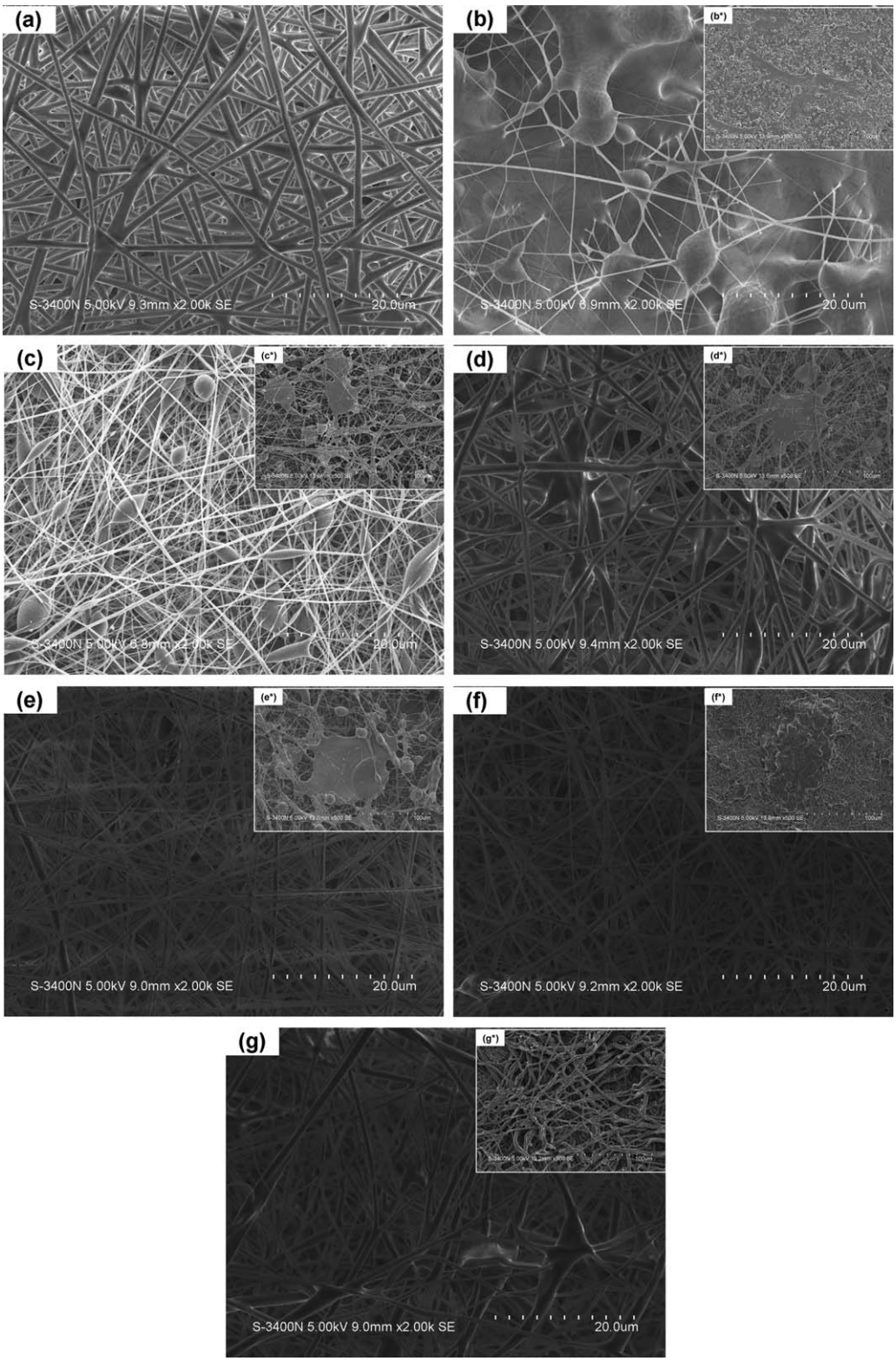

Figure 1. SEM images of micromorphology (a–g) and cell adhesion behavior (b*–g*) for electrospun nanofibers of polymer(s) with different compositions. (a) PLA, (b and b*) CS, (c and c*) PLA+CS, (d and d*) PLA+CS+1%TX-15, (e and e*) PLA+CS+2%TX-15, (f and f*) PLA+CS+3%TX-15, (g and g*) PLA+CS+4%TX-15. a*–g* show corresponding cell adhesion morphology observations of samples b–g cultured with human bone-marrow hMSCs for 3 days. (Scale a-g 20μm and a*–g* 100 μm).

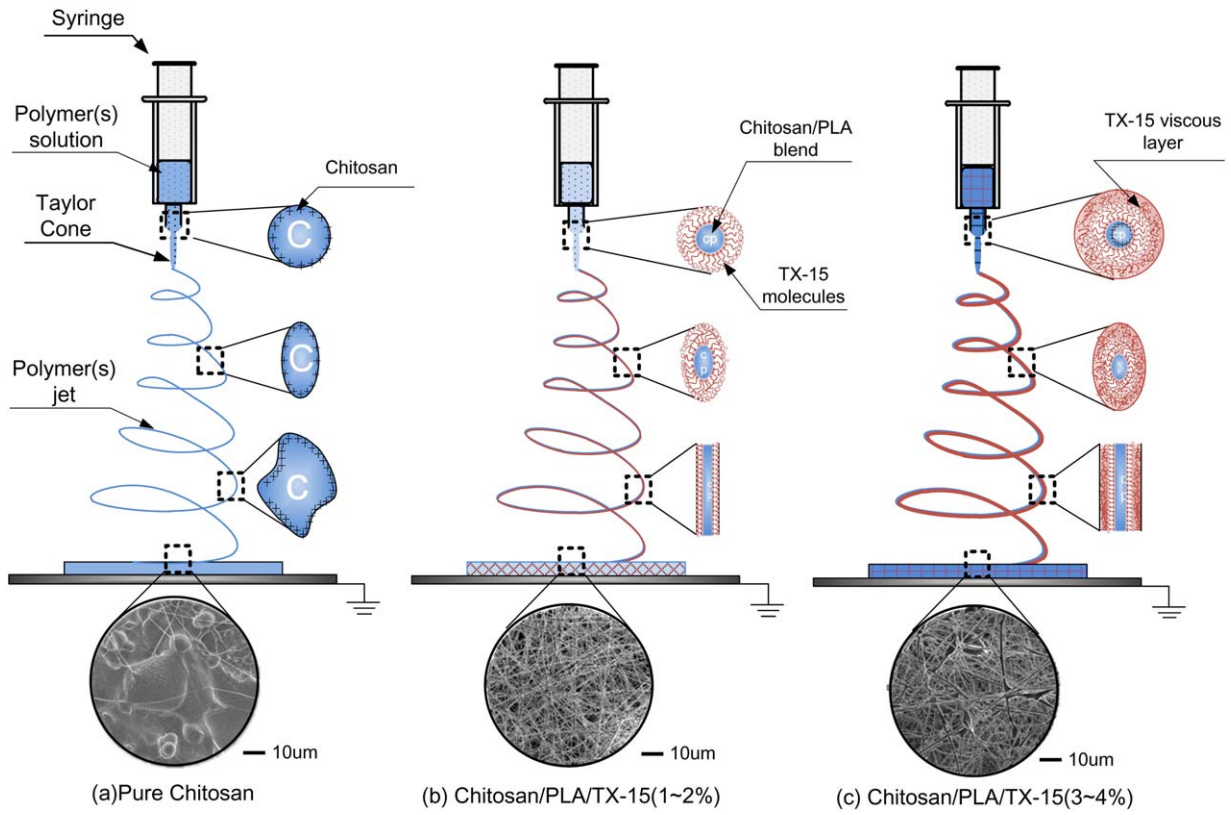

Figure 2. Schematic representation of nanofiber scaffold formation and TX-15 distribution in solutions and nanofibers: (a) pure CS droplets move through the capillary under an electric force and form a lamellar or drop-like deposition; (b) some TX-15 molecules migrate to the external surface and increase the charge density of the droplets, resulting in uniform nanofiber deposition; (c) too many TX-15 molecules adsorbed onto the droplets surface, result in increased viscosity of the solution and interference with solvent evaporation. [Color figure can be viewed in the online issue, which is available at wileyonlinelibrary.com.]

beading and resulting in nanofibers with smaller mean diameters, as shown in Figure 1(c–e). The diameter of CS/PLA blend solutions decreased from 450 ± 65 nm to 249 ± 52 nm when the TX-15 content was increased from 0% to 2% (Table I).

TX-15 is a nonionic surfactant that contains several hypophilic groups, including an hydroxyl group (—OH) and an ether linkage (—C—O—C—); such groups can form hydrogen bonds by combining with the —OH group derived from PLA and the amino groups of CS. Additionally, the hypophilic chains of TX-15 move randomly in solution; as such, they may convolve the CS/PLA molecular chains or cover the CS/PLA modular surface. These actions may reduce surface tension and improve the electrospinnability of composites. With respect to the pure CS solution, when the electrostatic force generated by the electrospin procedure overcomes the surface tension of the droplets, the charged emulsion droplets move vertically to complete their enrichment at the capillary tip [Figure 2(a)]. Upon application of the electrical field, the droplets were stretched into an elliptical shape and extended into a fine jet; moreover, the solvents were evaporated and the jet rapidly solidified. In the end, nanofibers were formed. As a surfactant, TX-15 has relatively high mobility in the electrospun polymer jet and can move to the gas–liquid interface, thus increasing the charge density of the droplets.[4] The overall tension in the nanofibers depends on the self-repulsion of the excess charges in the jet. Therefore, as the charge density increases with the addition of TX-15, the diameter of the final nanofibers becomes smaller [Figure 2(b); Table I]. As a result, addition of 2% TX-15 results in fine nanofibers with uniform morphology and an average fiber diameter of 249 ± 52 nm (Figure 1; Table I).

At excessively high solution concentrations of TX-15, electrospinning was difficult and uniform fiber formation of the polymers was poor. The diameter distribution of the nanofiber mats is shown in Table I. Diameters dramatically increased with increasing TX-15 concentration in the blend up to approximately 2%; structures became more lamellar in shape at concentrations near 4% [Figure 1(f,g)]. Similar findings were previously reported by Charernsriwilaiwat et al.[9] This phenomenon can be explained in terms of solution viscosity as listed in Table I. When the viscosity of the solution is increased, the formation of beads and the diameter of the nanofibers both increase.[9] Since TX-15 is a surfactant, it forms excessive hydrogen bonds with polymers if its concentration is too high; as a result, it interferes with solvent evaporation. Such hydrogen bonding would gradually affect the viscosity of the emulsion [Figure 2(c)]. Increased viscosity of the emulsion would decrease electrospinnability, resulting in a more bead-like structure and larger diameter of the nanofibers [Figure 1(f,g)].

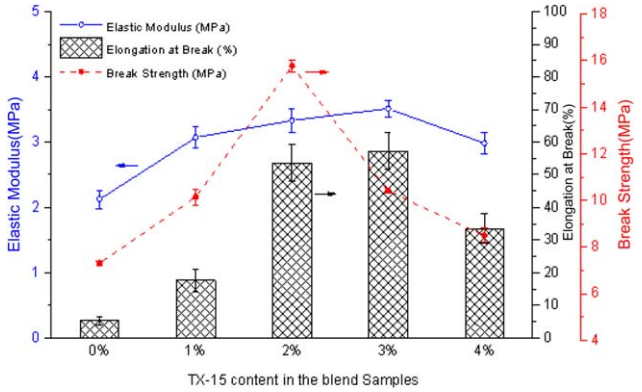

Figure 3. Mechanical properties of CS/PLA/TX-15 blends with different concentrations of surfactant. (c) Blends with 0% TX-15, (d) blends with 1% TX-15, (e) blends with 2% TX-15, (f) blends with 3% TX-15, and (g) blends with 4% TX-15. [Color figure can be viewed in the online issue, which is available at wileyonlinelibrary.com.]

Hydrophilicity of Nanofibers. Contact angle measurement, a convenient surface-sensitive technique, was used to monitor the extent of surface modification. In this study, water was used as the medium for contact-angle measurements. As expected, the surface hydrophobicity of PLA fiber films decreased upon introduction of CS (Table I). The static water contact angle of pristine PLA is $83.1 \pm 0.7°$. Blending with CS caused the value to decrease to approximately 72°. Furthermore, since TX-15 is a highly hydrophilic surfactant that is easily dissolvable in water, its presence in the PLA/CS composite nanofibers causes an increase in the hydrophilicity of the blend nanofibers. As listed in Table I, the contact angles decrease from $71.8 \pm 0.2°$ to $41.5 \pm 0.9°$ when the concentration of TX-15 is raised from 0% to 4%.

We also measured the dynamic swelling behavior, which was consistent with the contact angle measurement (Table I). CS is a hydrophilic biopolymer with a swelling rate of 57.8% at 72 h in this study. However, the hydrophilicity of CS changed remarkably after the introduction of PLA, which represents relative hydrophobicity. After incubation with water for 72 h, the CS fiber film swelling rate was decreased to 43.3%; in the presence of PLA, the swelling rate was 34.2%. We also found that in the absence of TX-15, there was an increased ability of water to penetrate the fiber network; this is likely because the PLA/CS/TX-15 scaffolds showed considerably higher swelling rates than the PLA/CS scaffolds. The equilibrium swelling point for CS/PLA at 24 h was 39.1% (Table I). For blend polymers containing 4% TX-15, the electrospun scaffolds reached high equilibrium swelling values of 62.4% within the first 24 h of the experiment; this was followed by a steady and continuous increase over 72 h. As expected, water uptake was more pronounced for the more hydrophilic fabrics.

The nonionic surfactant TX-15 contains an alkyl chain that serves as the hydrophobic moiety and a polyoxyethylene ether (POE) chain that serves as the hydrophilic moiety. TX-15 has been extensively studied due to its good solubilization properties and high surface activity.[33] Consistent with this, we found that the introduction of TX-15 into PLA/CS blend nanofibers increased the hydrophilicity of the materials.

Variations in fiber density were examined by SEM [Figure 1(c–g)]. Density increased with increasing TX-15 concentration, and this resulted in a higher surface area of connected networks, which improved water permeability and moisture sorption of the matrix.[34]

Scaffold Mechanical Properties. As shown in Figure 1(b), pure CS film showed a lamellar morphology and a bead-like structure. Additionally, it was very brittle and could not be easily removed from the collector target. Because of this, it could not be mechanically tested. The electrospun fiber mats fabricated from CS/PLA and CS/PLA/TX-15 were more flexible and could be removed more easily. Thus, compared to pure CS film, the other sample fiber mats could be easily used in mechanical studies.

Mechanical properties, including break strength, elastic modulus, and elongation at break, of different blend ratios of TX-15 in CS/PLA films are shown in Figure 3. These mechanical properties display a definite trend. The break strength gradually increases with increasing TX-15 when the ratio of TX-15 is low. However, once the TX-15 ratio is increased above 4%, the break strength significantly decreases. Similar results were obtained for elastic modulus and elongation at break. Although CS/PLA with 3% TX-15 was harder (elastic modulus, 3.51 ± 0.12 MPa) and tougher (elongation at break, $57.27 \pm 5.62\%$), CS/PLA with 2% TX-15 was stronger (break strength, 15.77 ± 0.24 MPa) (Figure 3). Taken together, the properties of the polymer are largely influenced by TX-15 concentration.

As a surfactant, TX-15 serves as a "bridge" in the blend system, combining different polymer phases and improving the miscibility of the blend polymers. Chen et al.[28] reported that phase boundary properties affect the mechanical properties. Here, we find that the mechanical properties increase with improved miscibility of the CS/PLA fiber. However, once the surfactant concentration is too high, TX-15 forms an individual phase within

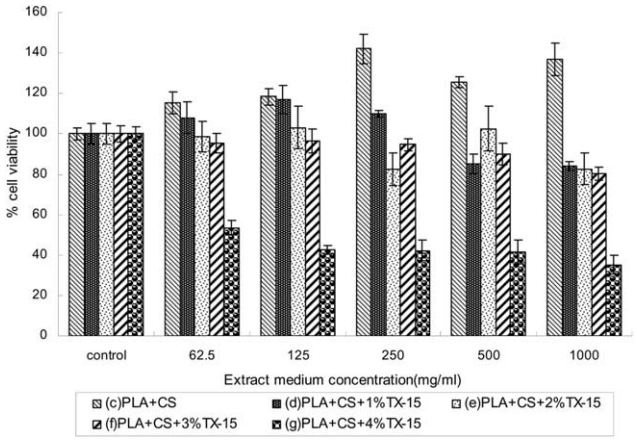

Figure 4. *In vitro* cytotoxicity of PLA/CS/TX-15 blend nanofibers with different TX-15 concentrations against human bone marrow hMSCs at 72 h. Untreated cells served as controls.

the mixture [Figure 2(c)] and interferes with the miscibility of the blend.

***In Vitro* Cell Adhesion and Proliferation.** *In vitro* cell adhesion and proliferation on the fiber mats were evaluated in cultured hMSCs over a 3-day period. Because of their differentiation potential, hMSCs were used for comparing the biocompatibility of different nanofiber mats.[30] Cytotoxicity in the presence of CS/PLA/TX-15 at different TX-15 ratios ranging from 0% to 4% are shown in Figure 4.

There was a significant decrease in cell viability when the hMSCs were incubated with various concentrations of extraction media from nanofiber mats of 4% TX-15. Consistent with this, only a few cells were observed in the matrix from sample (g) by SEM observation [Figure 1(g*)]. Cell viability was not significantly altered by any of the other sample mats [Figure 4(c–f)]. SEM observation also showed that cells had spread well onto the fiber mats [Figure 1c*–f*] with a high level of cell/scaffold interaction; this was demonstrated by the numerous pseudopodia and cell secretions that emerged. A scaffold must be able to promote the normal cellular state. We show this here, as the CS/PLA/TX-15 nanofiber mats are nontoxic. Thus, they have the potential to be developed as drug delivery carriers or skin tissue engineering scaffolds.

CONCLUSIONS

The CS/PLA/TX-15 blend nanofibers have been successfully fabricated by electrospinning. The weight ratio of TX-15 in the blend affects the basic physical characteristics, such as diameter and morphology. Uniform and smooth morphology of the nanofibers, with a narrow diameter distribution of approximately 249 ± 52 nm, were obtained with a TX-15 ratio of 2%. Hydrophilicity tests suggested that the addition of TX-15 increases the hydrophilicity of the nanofibers. Mechanical studies demonstrated that the electrospun fiber mats displayed better tensile mechanical properties when the ratio of TX-15 was approximately 2%–3%. Furthermore, cytotoxocity tests showed that CS/PLA/TX-15 nanofiber mats were safe and nontoxic toward hMSCs. In total, TX-15 is an effective surfactant to improve the electrospinnability of CS. This assay could have potential application for drug delivery or tissue engineering.

ACKNOWLEDGMENTS

This project was supported by the National Natural Science Foundation of China (Grant No. 31100673) and the Shanghai Municipal Natural Science Foundation (Grant No. 11ZR1435800). The authors sincerely thank the Shanghai City Board of education innovation project (Grant No. 12YZ162), the Shanghai Committee of Science and Technology through the nano-technology promotion project (0952nm03400) and the grant for composite materials from Shanghai Institute of Technology (10210Q140001) for their support as well.

REFERENCES

1. Gingras, M., Paradis, I., Berthod, F. *Biomaterials* **2003**, *24*, 1653.
2. BÖttcher-Haberzeth, S., Biedermann, T., Reichmann, E. *Burns* **2010**, *36*, 450.
3. May, A. K. *Surg. Clin. North Am.* **2009**, *89*, 403.
4. Li, X. Q., Su, Y., Liu, S. P., Tan, L. J., Mo, X. M., Sramakrishna, S. *Colloid Surface B* **2010**, *75*, 418.
5. Rosso, F., Giordano, A., Barbarisi, M., Barbarisi, A. *J. Cell. Physiol.* **2004**, *199*, 174.
6. Kim, B. S., Park, I. K., Hoshiba, T., Jiang, H. L., Choi, Y. J., Akaike, T., Cho, C. S. *Prog. Polym. Sci.* **2011**, *36*, 238.
7. Shalumon, K. T., Anulekha, K. H., Girish, C. M., Prasanth, R., Nair, S. V., Jayakumar, R. *Carbohyd. Polym.* **2010**, *80*, 413.
8. Aluigi, A., Varesano, A., Montarsolo, A., Vineis, C., Ferrero, F., Mazzuchetti, G., Tonin, C. *J. Appl. Polym. Sci.* **2007**, *104*, 863.
9. Charernsriwilaiwat, N., Opanasopit, P., Rojanarata, T., Ngawhirunpat, T., Supaphol, P. *Carbohyd. Polym.* **2010**, *81*, 675.
10. Rho, K. S., Jeong, L., Lee, G., Seo, B. M., Park, Y. J., Hong, S. D., Roh, S., Cho, J. J., Park, W. H., Min, B. M. *Biomaterials* **2006**, *27*, 1452.
11. Heydarkhan-Hagval, S., Schenke-Layland, K., Dhanasopon, A. P., Rofail, F., Smith, H., Wu, B. M., Shemin, R., Beygui, R. E., MacLellan, W. R. *Biomaterials* **2008**, *29*, 2907.
12. Ji, W., Yang, F., van den Beucken, J. J. J. P., Bian, Z., Fan, M., Chen, Z., Jansen, J. A. *Acta Biomater.* **2010**, *6*, 4199.
13. Agawal, S., Wendorff, J. H., Greiner, A. *Polymer.* **2008**, *49*, 5603.
14. Kim, I. Y., Seo, S. J., Moon, H. S., Yoo, M. K., Park, I. Y., Kim, B. C., Cho, C. S. *Biotechnol. Adv.* **2008**, *26*, 1.
15. Min, B. M., Lee, S. W., Lim, J. N., You, Y., Lee, T. S., Kang, P. H., Park, W. H. *Polymer* **2004**, *45*, 7137.
16. Chen, J. W., Tseng, K. F., Delimartin, S., Lee, C. K., Ho, M. H. *Desalination* **2008**, *233*, 48.
17. Geng, X., Kwon, O. H., Jang, J. *Biomaterials* **2005**, *26*, 5427.
18. Homayoni, H., Ravandi, S. A. H., Valizadeh, M. *Carbohyd. Polym.* **2009**, *77*, 656.
19. Gu, B. K., Park, S. J., Kim, M. S., Kang, C. M., Kim, J. I., Kim, C. H. *Carbohyd. Polym.* **2013**, *97*, 65.
20. Han, J., Zhang, J., Yin, R., Ma, G., Yang, D., Nie, J. *Carbohyd. Polym.* **2011**, *83*, 270.
21. Giri, T. K., Thakur, A., Alexander, A., Ajazuddin, Badwaik, H., Tripathi, D. K. *Acta Pharm. Sin. B.* **2012**, *2*, 439.
22. Sonseca, A., Peponi, L., Sahuquillo, O., Kenny, J. M. Giménez, E. *Polym. Degrad. Stab.* **2012**, *97*, 2052.
23. Van der Schueren, L., Steyaert, I., Schoenmaker, B. D., Clerck, K. D. *Carbohyd. Polym.* **2012**, *88*, 1221.
24. Xu, J., Zhang, J., Gao, W., Liang, H., Wang, H., Li, J. *Mater. Lett.* **2009**, *63*, 658.
25. Pakravan, M., Heuzey, M. C., Ajji, A. *Polymer.* **2011**, *52*, 4813.
26. Li, A. D., Sun, Z. Z., Zhou, M., Xu, X. X., Ma, J. Y., Zheng, W., Zhou, H. M., Li, L., Zheng, Y. F. *Colloid Surface B* **2013**, *102*, 674.

27. Kriegel, C., Kit, K. M., McClements, D. J., Weiss, J. *Polymer* **2009**, *50*, 189.

28. Chen, C. C., Chueh, J. Y., Tseng, H., Huang, H. M., Lee, S. Y. *Biomaterials* **2003**, *24*, 1167.

29. Shan, X. Q., Yuan, Y., Liu, C. S., Xu, F., Sheng, Y. *Soft Matter.* **2009**, *5*, 2875.

30. Dargaville, B. L., Vaquette, C., Rasoul, F., Cooper-White, J. J., Campbell, J. H., Whittaker, A. K. *Acta Biomater.* **2013**, *9*, 6885.

31. Yan, S., Changsheng, L., Yuan, Y., Xinyi, T., Fan, Y., Xiaoqian, S. Huanjun, Z., Feng, X. *Biomaterials* **2009**, *30*, 2340.

32. Urbina, M. C., Zinoveva, S., Miller, T., Sabliov, C. M., Monroe, W. T., Kumar, C. S. S. R. *J. Phys. Chem. C* **2008**, *112*, 11102.

33. Chen, Z. X., Deng, S. P., Li, X. K. *J. Colloid. Interface Sci.* **2008**, *318*, 389.

34. Pereda, M., Amica, G., Rácz, I., Marcovich, N. E. *J. Food. Eng.* **2011**, *103*, 76.